Design of a Fan-Test-Facility with axial flow and crosswind capabilities

Jan-Hendrik Krone* and Jens Friedrichs,†

TU Braunschweig, Institute of Jet Propulsion and Turbomachinery, 38108 Braunschweig, Germany

Abstract

Providing capabilities for investigations on future fan systems a new test facility layout was developed which takes all fan system components together with a nacelle into accout. The main development criteria was to include fan performance and internal as well as external nacelle flow in order to obtain all interaction effects playing a dominant role for future high bypass fan systems. It was considered to vary the pitch angle of the fan model but due to the high power fan drive such a setup is too complex. However, in order to provide critical conditions such as angle of attack a new crosswind concept has been developed. This concept uses a blocking flow beside the fan model deflecting the main flow and thus leading to an angle of attack relative to the nacelle. The aim of this numerical study was to determine whether velocity and angle distributions provided by this concept lead to representative diffusor inlet separations which in turn affect fan performance. The results show that the deflection of main flow leads to angles of attack up to 14°. Further simulations including a NACA1 nacelle have approved that the concept is able to generate diffusor inlet separations of representative dimensions.

Nomenclature

b^*	Half duct width	[m]
Ma_∞	Inlet mach number	[-]
$\dot{m}$	Mass flow	[kg/s]
v_{cw}	Crosswind velocity	[m/s]
v_{res}	Resulting velocity	[m/s]
v_x	Velocity in x-direction	[m/s]
v_z	Velocity in z-direction	[m/s]
v_∞	Test section inlet velocity	[m/s]
α	Angle of attack	[°]
μ	Bypass ratio	[-]

*Research scientist.

†Professor.

B1 to B12	Blowers
CFD	Computational Fluid Dynamics
CW	Crosswind
FD	Fan drive
L1	Evaluation duct height L1
L2	Evaluation duct height L2
NACA	National Advisory Committee for Aeronautics
P1	Evaluation plane 1
P2	Evaluation plane 2
P3	Evaluation plane 3
SC	Settling chamber
TO	Test object
TS	Test section

1 Introduction

Airline operators are continually confronted with rising fuel costs and more strict noise exposure guidelines. In order to meet these requirements, jet engine manufacturers are challenged to furthermore improve overall engine efficiency and to decrease noise emissions. Over the years, significant improvements of overall engine efficiency were achieved by increasing the propulsive efficiency which depends on the difference of engine exit and inlet flow velocity. For a small difference and thus low exit velocities propulsive efficiency is improved and as a consequence specific fuel consumption decreases. While the thrust directly depends on that velocity difference a decrease in exit velocity has to be compensated by an increased total engine mass flow. This in turn implies a high bypass ratio μ and thus large fan diameters.

In general, increasing the fan diameter leads to a decrease in fan pressure ratio. The reason for this is a limitiation of blade tip speed ensuring adequate aerodynamic losses. Based on this, an increase in fan diameter causes a decrease in rotational speed and thus a decrease in pressure ratio. The historical development of fan pressure and bypass ratios of commercial turbofan engines are illustrated by Mazzawy [1]. According to this study, pressure ratios have decreased from values around 1.8 to approximately 1.4. In general, for low fan pressure ratios the operation stability mainly depends on the inlet conditions provided by the upstream diffusor. Especially at critical conditions such as crosswind or angle of attack during climb the diffusor flow has a major influence on fan blade performance and stability. Since for a low pressure ratio the whole fan system becomes more susceptible to aerodynamic instabilities, the interaction of diffusor flow and fan blade performance is a major design criteria for the development of future high bypass turbofan engines.

Experimental investigations taking external nacelle flow as well as diffusor flow into account were carried out for example by Quemard et al. [2]. These so-called air intake tests have determined performances of a representative nacelle inside of a classical windtunnel. Critical conditions such as crosswind were simulated by an angle of attack of the nacelle relative to the incoming flow. The bypass mass flow itself was simulated by a secondary air system providing the required mass flow defined by the scale of the nacelle. Because of the focus on external and internal nacelle flow rotating components were not considered within these investigations and therefore fan blade performance during critical conditions was not obtained.

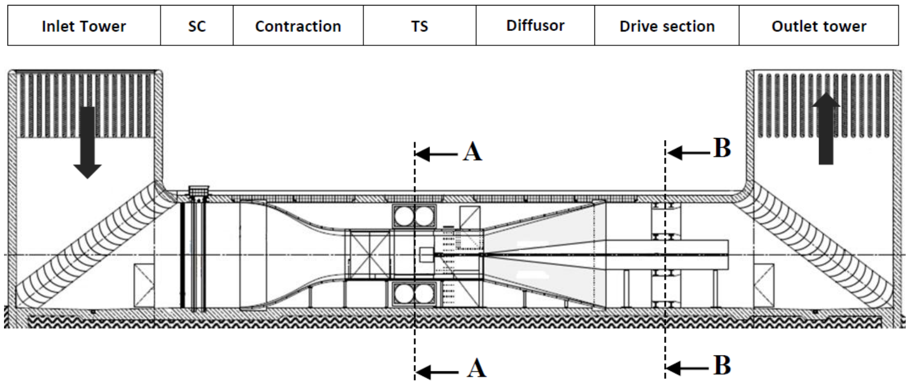

Figure 1: Fan-Test-Facility layout

In order to provide capabilities for tests of low pressure ratio fan systems at realistic critical conditions, a new facility layout was developed at the Institute of Jet Propulsion and Turbomachinery. The combination of a high power fan test rig including all fan system components and classical windtunnel capabilities will provide the possibility to obtain all interaction effects occuring inside of a fan system. The drive concept of this facility allows to test fan models of current turbofan engines with a scale in the range of 1:3 to 1:5 but due to the high power drive the fan model is not pitchable. Still providing the possibility to generate crosswind conditions a new crosswind concept has been developed. In order to determine the range of achievable inlet distortions as well as quantitative offsets to above mentioned experimental setups this study presents the results of numerical concept validation.

2 Facility layout

2.1 Capabilities

Basically, the facility layout represents a U-Type jet engine test bed, shown schematically in Fig. 1. Flow enters the facility through the inlet tower and is turned by corner vanes leading to a settling chamber (SC) including screens and a honeycomb improving the flow quality. Further downstream the contraction leads to the test section (TS) which contains the fan model and the crosswind duct which is illustrated in Fig. 2 (left). Crosswind enters the test section through a door beside the fan model and on the opposite side flow enters into the recirculation duct powered by four blowers. The main advantage of this closed loop crosswind duct is to operate on the respective static pressure level defined by the test section flow velocity. The mechanism of this experimental setup is described below. Downstream of the test section the diffusor leads to the drive section including an array of eight blowers (Fig. 2 (right)) as well as an electric motor drive powering the fan. Downstream of the drive section the second corner vane row guides the flow into the outlet tower. Because of noise emission guidelines both towers contain acoustic baffles. With these capabilities the facility provides following testing setups:

1. Fan performance investigations at $Ma_\infty = 0$
2. Fan performance investigations at axial incoming flow up to $Ma_\infty = 0.2$
3. Fan performance investigations at crosswind conditions

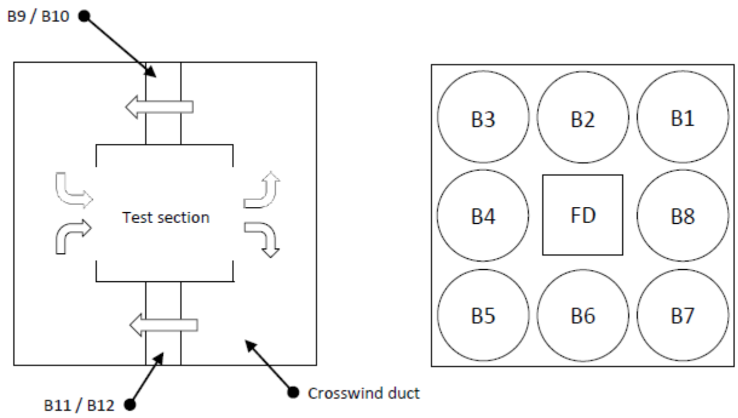

Figure 2: Section A-A (left), section B-B (right)

2.2 Crosswind concept

As mentioned above the test section contains the crosswind duct providing the possibility of the generation of critical fan inlet conditions. Fig. 3 illustrates the principle of the crosswind concept. The basic idea is to produce a blocking area developing from the crosswind inlet door leading to a deflection of the incoming flow v_∞. This deflection in turn causes an angle of attack α of the resulting velocity v_{res} relative to the axial direction. If the achievable angle of attack is large enough diffusor inlet seperations will occur. First step during numerical concept validation was to determine velocity and angle distributions at several planes within the area affected by the deflection. Probably, this crosswind concept will produce non-uniform velocity and angle distributions differing signficantly compared to a uniform angle of attack. Therefore, the objective was to determine velocity and angle offsets relative to the case of a uniform incoming flow and furhermore to carry out the optimum test object position within the test section.

3 Simulation setup

3.1 Calculations without test object

In order to determine the interaction mechanism of the main flow and the crosswind flow numerical investigations were carried out. Establishing a comparsion between the crosswind concept and a uniform angle of attack was achieved by neglecting the fan as a test object. For reasons of numerical robustness and complexity the CFD model was further reduced to the test section, see Fig. 4. The recirculation duct which provides the connection between the crosswind doors is not included as well. The CFD model consists of the test section duct walls with two inlet and two outlet boundary conditions. Green and blue colored boundary locations in Fig. 4 represent the test section inlet and outlet. On these planes the boundary conditions were set to a velocity inlet and a static pressure outlet. Magenta and yellow colored boundary locations represent the crosswind inlet and outlet planes defined as equal mass flow conditions ($\dot{m}_{CW,in} = \dot{m}_{CW,out}$). The mesh used for these simulations is a multiblock structured mesh and

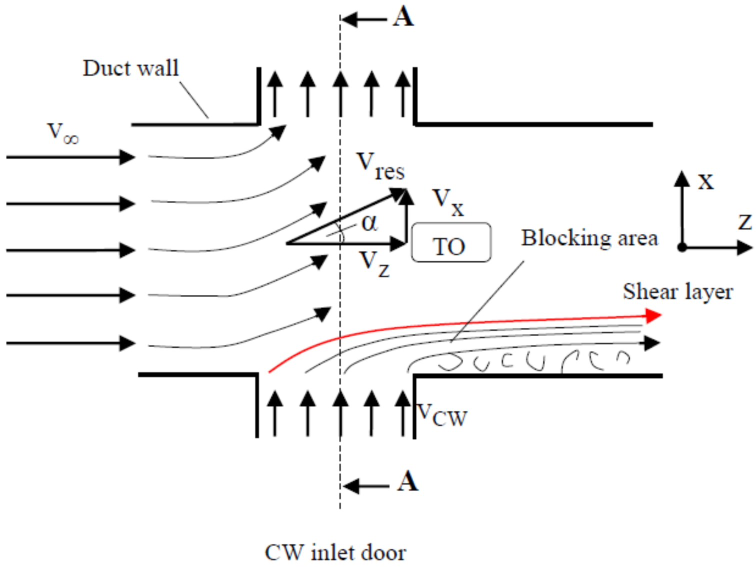

Figure 3: Generating of angles of attack by flow interaction

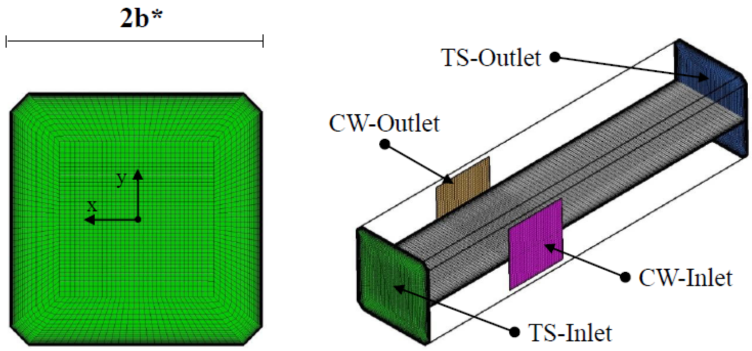

Figure 4: Structered mesh of the test section

has about 600.000 nodes. The analysis type was steady state, the turbulence model was set to standard SST and the solver was ANSYS CFX.

The planes on which flow evaluations were carried out are presented in Fig. 5 (left). While plane 1 (P1) and 3 (P3) are located at the crosswind door edges, plane 2 (p2) is placed in the middle. Fig. 5 (right) defines two lines on each of the planes (L1 and L2). L1 is located at a relative duct height of 50 % whereas L2 represents the outer diameter of a representative nacelle.

3.2 Calculations with test object

A further crosswind validation step was to account for a representative test object inside of the test section. The objective was to determine whether angle distributions obtained at validation step one will lead to diffusor inlet separation. The nacelle contour was defined according to NACA1 design criterias with a fan diameter about 0.7m. As usual for numerical investigations on nacelle intake simulations the fan plane boundary condition was shifted downstream. An illustration of main test object dimensions is presented in Fig. 6 (a). The structured mesh as shown in Fig. 6 (b) was generated using ICEM CFD and has about 2 million nodes. With respect to step one validation results the diffusor entry plane is located at P2 since it provides most uniform inlet conditions.

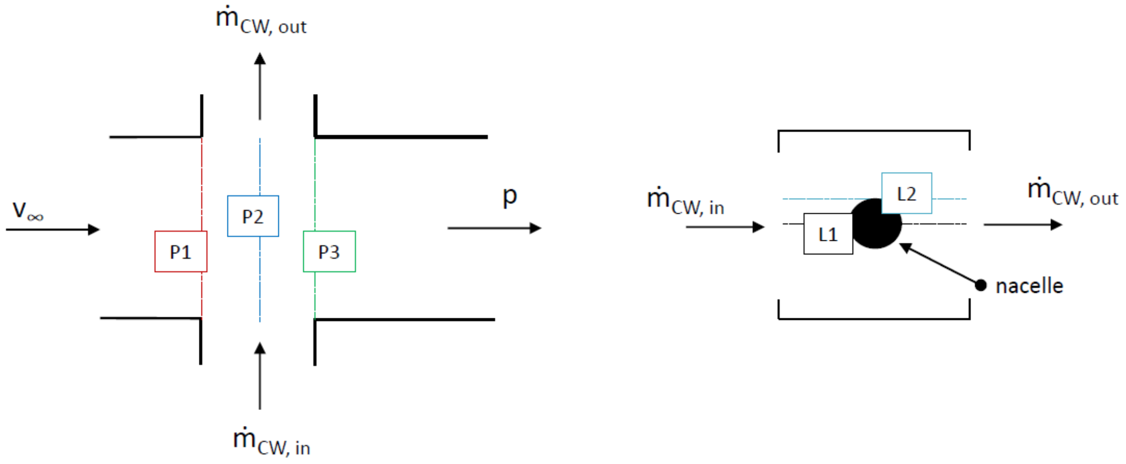

Figure 5: Boundary conditions and locations of flow evaluation

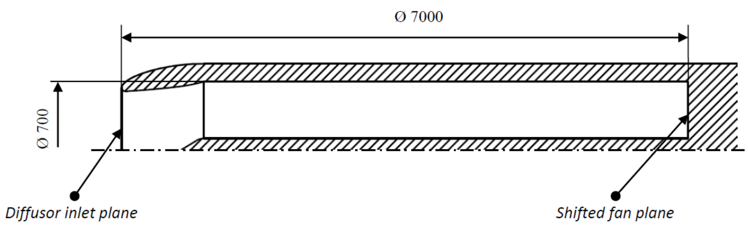

(a) Dimensions

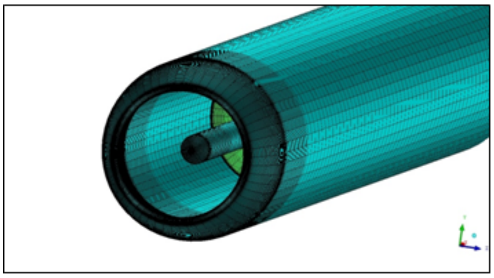

(b) Structured mesh

Figure 6: Mesh of a representative test object (Dimensions in millimeters)

4 Results

4.1 Calculations without test object

Velocity and angle distributions on each plane at $Ma_\infty = 0.2$ and a normalized crosswind mass flow of 3% are illustrated in Fig. 7. The normalized crosswind mass flow is defined as the ratio of the crosswind mass flow and the total mass flow entering the test section inlet. In terms of comperability the absolute velocity v_{res} is normalized by the incoming velocity v_∞. While the characteristic of the velocity distribution depends on the plane there is no significant difference between level 1 (L1) and level 2 (L2). Except P2 all distributions show a significant drop in velocity towards $x/b^* = -1$ caused by the blocking area. Because of P2 located upstream of the blocking area there is no drop in velocity. Instead flow is deccelerated resulting in the presented distribution. The area of major interest is bordered by blue lines since it represents the area of a test object. Within these borders the most uniform velocity profile is obtained for P2. Compared to the incoming flow velocities have increased. The reason for this is that the blocking area reduces the effective test section area and thus according to continuity main flow

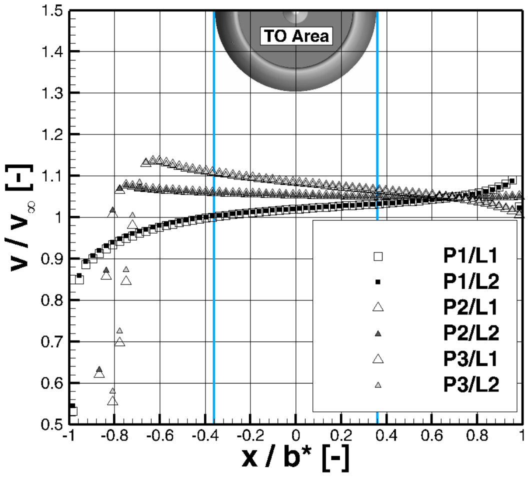

(a) Absolute velocity

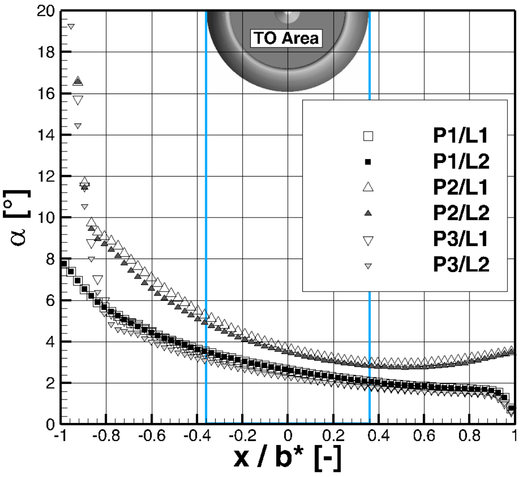

(b) Angle of attack

Figure 7: Results for $Ma_\infty = 0.2$ and 3% crosswind massflow

is accelerated. Fig. 7 (b) shows the respective distribution of angle of attack. In general, from $-1 < x/b^* < 0.4$ angle of attack significantly decreases. This is due to the deflection effect which is gained towards the blocking area. Hence, as supposed angle distributions are not free of gradients for the crosswind concept of this facility. The highest level of angles in the range of 3° to 5° is provided by P2. Since P2 also provides the most uniform velocity profile it is supposed to represent the optimum test object location.

Increasing the crosswind mass flow up to 9% leads to velocity and angle distributions shown in Fig. 8. According to a crosswind mass flow of 3% equal plane characteristics were obtained but in an amplified manner. Due to an increased blocking area, the point of velocity drop has moved towards the test object area. On P3 this turning point which represents the shear layer between main and crosswind flow is approximately located at the blue border. What has to be prevented is a setup for which this shear layer enters the fan. Since such an inlet profile does not match realistic inlet conditions the case of P3 represents a limit. Obviously, the most uniform velocity profile occurs on P2 as obtained for the lower crosswind mass flow. While an increase of the blocking area reduces the effective main flow area the velocity level has further increased at all planes.

Corresponding evaluations of angle of attack are illustrated in Fig. 8 (b). An increase in crosswind mass flow has increased both angle level and angle gradient. The maximum angle within the test object area is obtained on P2 and is about $\alpha = 14°$. For this area the range of angle of attack at P2 is about 5° which is considerably more than for the 3% crosswind mass flow. Hence, the main conclusion of this validation step is that for constant inlet mach number main flow velocity and angle gradient are a function of crosswind mass flow.

4.2 Calculations with test object

Fig. 9 shows mach number contour plots on the fan plane for both crosswind mass flows. A relative mass flow of 3% results in a small separation area at the 3 o'clock position. At 9% crosswind mass flow the separation area has significantly increased. The radial extension is roughly half of the duct height. Furthermore, the calculations predict an area of increased flow

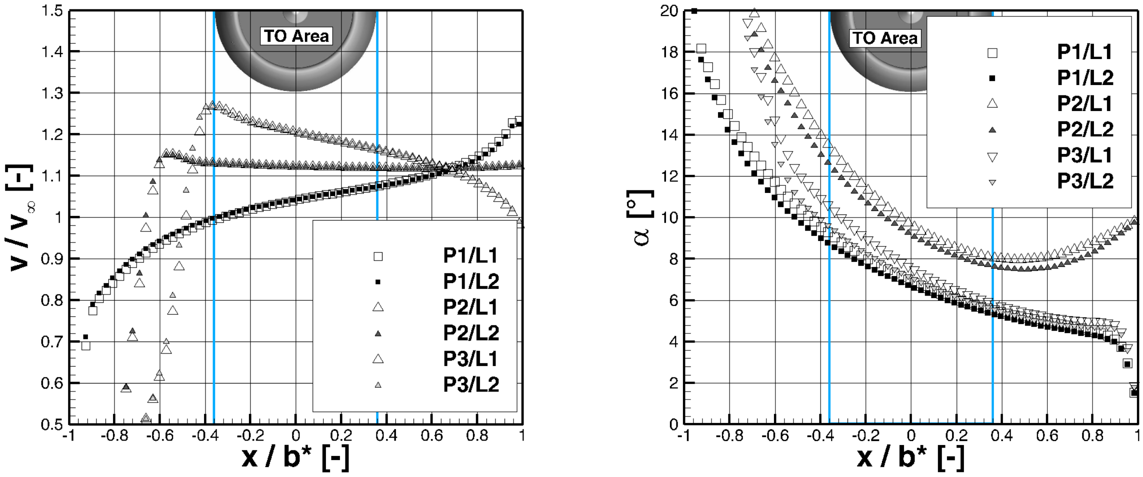

(a) Absolute velocity

(b) Angle of attack

Figure 8: Results for $Ma_\infty = 0.2$ and 9% crosswind massflow

velocity located at the 3 o'clock position indicating an area of recirculation. The large area of separation and recirculation reduces the remaining throat area leading to increased main flow mach numbers up to 0.75.

Regardless of the difference between the new crosswind concept and classical windtunnel investigations numerical simulations predict representative diffusor separations. Hence, it will be possible to investigate fan performance during realistic critical inlet conditions and thus the interaction of internal and external nacelle flow.

5 Conclusion

With regard to experimental investigations on future high bypass fan systems a new test facility layout has been developed including all fan components as well as the possibility to generate an incoming flow mach number up to 0.2. Fan performance at critical inlet conditions is of great importance for future fan systems but due to the high power of the fan drive the pitch angle of the test object is not adjustable. However, providing not only axial incoming flow but also critical conditions such as crosswind a new concept has been developed. The basic concept principles are as follows:

1. Incoming flow v_∞ is deflected by an additional mass flow entering the test section beside the fan model

2. Deflection of main flow leads to an angle of attack α of the resulting velocity v_{res}

3. Angle of attack produces diffusor inlet separations as obtained for fan operation during crosswind

The concept validation has shown that it is possible to generate typical diffusor inlet separations. Therefore, the facility provides capabilities of investigations on fan performance during

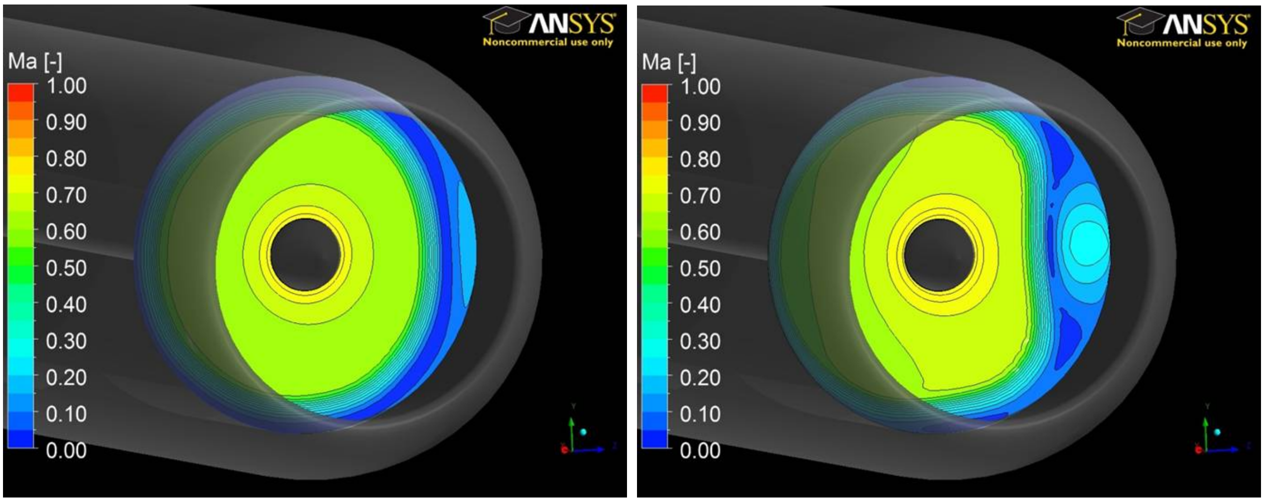

(a) 3% crosswind mass flow

(b) 9% crosswind mass flow

Figure 9: Mach number contour plots on fan plane

zero mach number, axial flow up to $Ma = 0.2$ and flow angles up to $\alpha = 14°$ representing critical conditions at take off. The major difference compared to classical air intake test is that for such a crosswind concept incoming velocity and angle profiles are not free of gradients. For this reason, further investigations have to determine the correlation between a uniform incoming flow and a crosswind condition provided by the new facility. Another idea is to generate non-uniform crosswind massflows which in turn could generate more uniform absolute velocities of the main flow.

References

[1] Mazzawy, R.S.: "Performance Study for Benefits of Variable Pitch Composite Fan". Proc. of ASME Turbo Expo, Glasgow, UK, 2010.

[2] Quemard, C. et al.: "High Reynolds Number Air Intake Tests in the Onera F1 and S1MA Wind-Tunnels". France, 1996.